

Spontaneous nucleation of microtubules

D. Kuchnir Fygenon,^{1,*} H. Flyvbjerg,^{1,2,3,†} K. Sneppen,¹ A. Libchaber,^{1,*} and S. Leibler^{1,‡}

¹Physics Department, Princeton University, Princeton, New Jersey 08544

²The Isaac Newton Institute for Mathematical Sciences, Cambridge CB4 0EH, England

³CONNECT, The Niels Bohr Institute, DK-2100 Copenhagen Ø, Denmark

(Received 17 October 1994)

The spontaneous nucleation of individual microtubules from tubulin dimers is observed directly under conditions of marginal nucleation. The results are compared with measurements of bulk turbidity following a deep quench [W. A. Voter and H. P. Erickson, *J. Biol. Chem.* **259**, 10430 (1984)]. The size of the critical microtubule nucleus is 12 ± 2 tubulin dimers in the two regimes, but the assembly pathway is different.

PACS number(s): 87.22.Bt, 82.35.+t

I. INTRODUCTION

Tubulin is an important protein in the cytoskeleton of all eukaryotes. It is a dimer 8 nm long and 4 nm in diameter. It has a remarkable tendency to aggregate (or polymerize) into long and very rigid hollow rods called *microtubules*. Microtubules have a chiral, crystalline structure, that typically incorporates 13 longitudinal protofilaments of dimers, and can be long enough to span a cell (10–100 μm). The dynamics of tubulin polymerization is governed by periods of growth interrupted by periods of rapid shortening. This so-called *dynamic instability* creates a robust and reasonably fast mechanism that performs complicated tasks for the cell [1]. Many studies have helped to characterize dynamic instability [2–5] but little attention has been given to the phenomenon of microtubule nucleation [6,7].

In the present work, we study the spontaneous nucleation of microtubules *in vitro* in the limit of very slow and very fast nucleation rates. The rate of nucleation is a function of temperature T and concentration of tubulin C . At very low concentrations or temperatures ($C < 10 \mu\text{M}$, $T < 15^\circ\text{C}$), the rate is unmeasurably slow. At moderate concentrations or temperatures ($10 \mu\text{M} < C < 40 \mu\text{M}$, $15^\circ\text{C} < T < 30^\circ\text{C}$), individual nucleation events can be recorded by measuring the density of single microtubules directly under an optical microscope. Since microtubules are effectively one dimensional, they consume the supply of tubulin quite slowly. Thus their nucleation can be monitored for relatively long times and at modest rates by direct observation under an

optical microscope. Upon quenching to very high temperatures or concentrations, nucleation proceeds rapidly and direct observation is difficult. In this regime, observations of the solution turbidity are often used as a measure of the microtubule density.

This paper is organized as follows. First, we investigate marginal nucleation. We describe an experiment in which we monitor microtubule density directly at moderate temperatures and concentrations. Under these conditions nucleation proceeds at a constant rate, indicating that it is, effectively, a single-step process. Furthermore, the rate scales with the (12 ± 2) power of the tubulin concentration, indicating that the critical nucleus involves 12 ± 2 tubulin dimers. Next, we consider nucleation after a deep quench. We reanalyze turbidity data from an experiment by Voter and Erickson [7] in which concentrated tubulin solutions, containing a large amount of glycerol, were quenched to high temperatures. In this regime, the critical nucleus, while the same size, is formed via three or four metastable states. Finally, we show that glycerol alone is not responsible for the different nucleation pathways.

II. NUCLEATION NEAR ONSET

Microtubules are essentially one dimensional, which means they can grow to considerable lengths at modest densities without significantly depleting the concentration of tubulin. In the regime we call marginal nucleation, single microtubules are sparse and we can count them individually for long times (minutes to hours), even at moderate nucleation rates, using an optical microscope.

A. Experimental method

The experimental setup is identical to one described elsewhere [5,8]. Purified tubulin ($< 0.1\%$ contaminating protein by weight) in an aqueous solution (100 mM Pipes, pH 6.9) with excess guanosine 5'-triphosphate (GTP) (1 mM) and MgSO_4 (2 mM) is placed between a glass slide and coverslip and observed with an optical microscope. The microscope is equipped for differential interference

*Present address: Rockefeller University, 1230 York Avenue, New York, NY 10021.

†Present address: HLRZ c/o Forschungszentrum Jülich GmbH, D-52425 Jülich, Germany.

‡Also at the Department of Biology, Princeton University, Princeton, NJ 08544.

contrast (DIC) imaging with video enhancement. The sample temperature is controlled by fluid flowing through a collar around the oil-immersed objective and through the sample stage. To create rapid temperature changes ($\sim 15^\circ\text{C}/\text{min}$), we switch between fluids from two different temperature baths. The sample comes within 0.5°C of its final temperature in 2 min and requires another 10 min to equilibrate completely.

At the beginning of a measurement, the sample is held at 4°C for at least 25 min to assure that no microtubules are present. The temperature is then raised abruptly. We translate the sample to observe one or more independent fields of view, sweeping the focus through the full depth of the sample in each. A field of view is $22.5 \times 30 \mu\text{m}^2$ and usually $\sim 50 \mu\text{m}$ deep (~ 34 picoliters). The sample depth is limited by the working distance of the objective. We favor thick samples since they are least affected by the nonspecific absorption of tubulin to the glass surfaces [9]. However, because it takes time to sweep the focus as we make our measurement (~ 1 min/ $50 \mu\text{m}$), we reduce the sample thickness to $25 \mu\text{m}$ to measure the fastest nucleation rate.

For each focal sweep, we record the time and the number of microtubule ends. Since every nucleation event generates two ends, the number of nucleation events corresponds to half the number of microtubule ends. We bin the observations in time, choosing the bin width such that each bin includes, on average, one new end. Observations are limited to less than 2 h by the natural decay of tubulin *in vitro*. When the nucleation rate is slow, we repeat the measurement to observe a total of at least four microtubule ends. At moderate nucleation rates, however, observations are limited instead by the density of microtubules since visibility is impaired once there are more than ~ 30 microtubules per field of view. Even so, the concentration of tubulin dimers in solution is never depleted by more than $\sim 1\%$ of its initial value.

B. Results

We monitor the density of microtubule ends as a function of time at various tubulin concentrations (12 – $60 \mu\text{M}$) and temperatures (18 – 40°C). Figure 1 is a typical plot of the density of microtubule ends as it develops with time for $T = 18^\circ\text{C}$ and $C = 60 \mu\text{M}$. The density increases at a constant rate and then saturates.

Observations are limited to conditions for which the typical time between nucleation events in the observable volume (25 – 500 picoliters), τ , is on the order of minutes to hours. Since the rate of nucleation changes with temperature, it is possible to observe nucleation over a wide range of tubulin concentrations. The nucleation rate dependence on concentration is plotted for three different temperatures in Fig. 2. At each temperature, a power law fit gives

$$1/\tau \propto C^{12 \pm 2}, \quad (1)$$

where $1/\tau$ is the nucleation rate per unit volume.

To interpret these results, we invoke a simple model. Consider a subcritical aggregate of x tubulin dimers which grows or shrinks one dimer at a time with probabilities g and s , respectively. (Ignore events involving

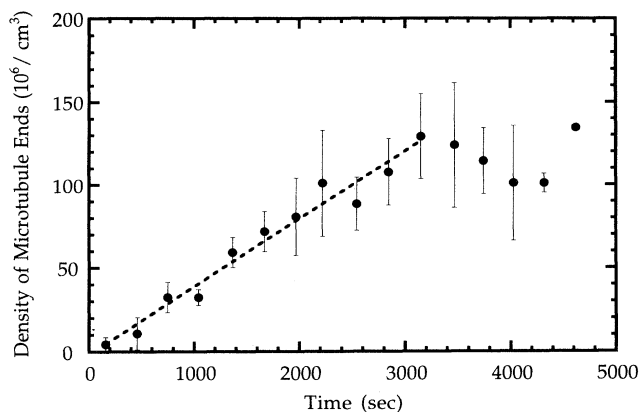


FIG. 1. Density of microtubule ends versus time for $C = 6 \mu\text{M}$ and $T = 18^\circ\text{C}$ as observed by video-enhanced DIC microscopy. The fit includes the first 55 min and gives a nucleation rate of $4 \times 10^4/\text{cm}^3 \text{sec}$. The saturation observed after this time is a result of aging of the sample. The nucleation rate is particularly sensitive to slight changes in the tubulin concentration ($1/\tau \propto C^{12}$), as is shown in Fig. 2.

more than one aggregate.) Both g and s must depend on the size of the aggregate so that subcritical aggregates are unstable and larger aggregates grow. The simplest such model has $g/s < 1$ for $x < N$ and $g/s > 1$ for $x \geq N$, where N is the size of the critical aggregate. It is reasonable to presume that g will be proportional to C while s should be independent of C . Therefore the critical size $x = N$ at which $g = s$ may decrease with increasing C . To first order $N = N(C) = N(C_0) - (1 - C/C_0)/f'$ where $f' = d(g/s)/dN$ is the slope of the size dependence of $g/s(C_0)$ at threshold. We assume this effect is negligible and consider g/s as a step function.

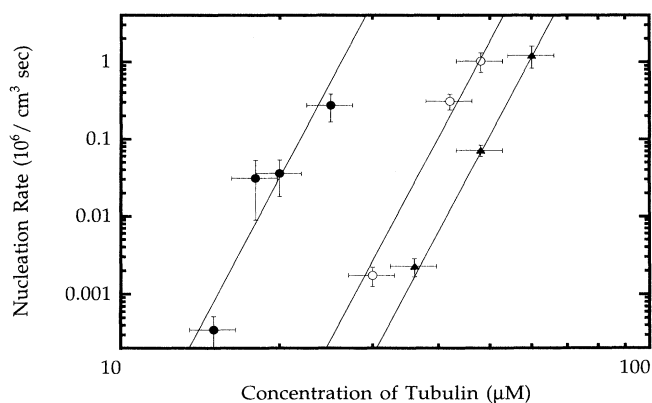


FIG. 2. Nucleation rate per unit volume versus concentration under conditions of marginal nucleation at three different temperatures: $T = 30^\circ\text{C}$ (solid circles), $T = 22^\circ\text{C}$ (open circles), and $T = 20^\circ\text{C}$ (triangles). The lines represent $1/\tau \propto C^{12}$. The error bars allow for an error of ± 2 in the exponent.

A constant nucleation rate implies a steady state population of subcritical aggregates, described by

$$gn(x) = sn(x+1) \text{ for } x < N-1, \quad (2)$$

where $n(x)$ is the concentration of aggregates of size x . From this we can deduce that nucleation within a volume V occurs at a rate

$$1/\tau = g \left(\frac{g}{s} \right)^{N-2} n(1) \propto C^N, \quad (3)$$

where $n(1) = C$ is the concentration of dimers.

This power law dependence agrees with the observations in Fig. 2. The exponent N does not change noticeably with concentration, consistent with our presumed steplike treatment of $g/s(x)$. We conclude that 12 ± 2 tubulin dimers are involved in the nucleus of a microtubule. Given an observed nucleation rate ($1/\tau \approx 0.1 \text{ sec}^{-1} \text{ cm}^{-3}$ when $C \sim 50 \mu M \sim 10^{16} \text{ dimers/cm}^{-3}$ and $T = 20^\circ \text{C}$) and applying an order of magnitude estimate of $g \sim 10^{2 \pm 1} \text{ dimers/sec}$ obtained from the measured absolute growth rate of a microtubule under these conditions [5], we find $g/s \approx 0.01$. This small value justifies ignoring processes involving multiple aggregates in the above model.

The model does not demand instantaneous condensation of N dimers, only subsequent aggregation. However, the value of g/s is so small in our case that the distinction between these two processes is meaningless.

III. NUCLEATION FAR FROM ONSET

We now turn to the regime of abundant nucleation in which microtubules are dense and begin depleting the bath of tubulin only minutes after nucleation starts. We reanalyze the results of an experiment by Voter and Erickson [7] in which tubulin solutions of different concentrations are quenched to high temperature (37°C) in the presence of glycerol. Microtubule mass density as a function of time is determined from the level of light scattered by a known volume of solution (turbidity). Some typical data are reproduced in Fig. 3(a).

We assume the measured turbidity is simply proportional to the amount of polymerized mass. This assumption is wrong for high concentrations of polymer [6] and for very short microtubules [10]. With respect to the first concern, the tubulin concentrations never exceed $19 \mu M$, and thus the turbidity was proportional to the polymer mass, as demonstrated in Fig. 2 of Ref. [7]. In addition, we are even further from the nonlinear regime since we use only the initial 10% of the turbidity data in our analysis.

As far as short microtubules are concerned, our assumption holds when the microtubules are longer than the wavelength of the light used to measure the turbidity $0.35 \mu m$ (Fig. A2 of Ref. [10]). In the most sensitive case (when the initial tubulin concentration is highest, $19.0 \mu M$), the growth velocity is about $0.1 \mu m/\text{sec}$ (extrapolated from measurements at lower concentrations [5]). Thus microtubules grow to $0.3 \mu m$ in length in about 3 sec. For comparison, the origin of time is defined with only 5 sec resolution because the initial temperature jump lasts

15 sec. A detailed analysis using the turbidity-mass relation from [10] shows that the error in identifying turbidity with total microtubule mass becomes insignificant for times $t > 3 \text{ sec}$ [11].

A. Analysis

Each curve shows a lag time followed by a fast rise in the microtubule mass density M . The fast rise is better observed on a logarithmic axis, as shown for a larger set of data in Fig. 3(b). The curves are parallel, meaning that M evolves in the same way for all initial concentrations: as a power law with an exponent between 4 and 5. The lag time, on the other hand, depends on the initial tubulin concentration C or, equivalently, on the final microtubule mass, $M_\infty \propto C$. If we define a characteristic time t_{10} , at which $M = M_\infty/10$, and plot this time versus M_∞ , we find $t_{10} \propto C^{-3}$, as illustrated in Fig. 4.

These results can be interpreted with some key modifications to our previous simple model. The details are given in the Appendix. Briefly, the fact that the nucleation rate accelerates over time means that the population of subcritical aggregates is not steady state. Equation (2) must therefore be replaced by a set of coupled differential equations describing temporal behavior of the

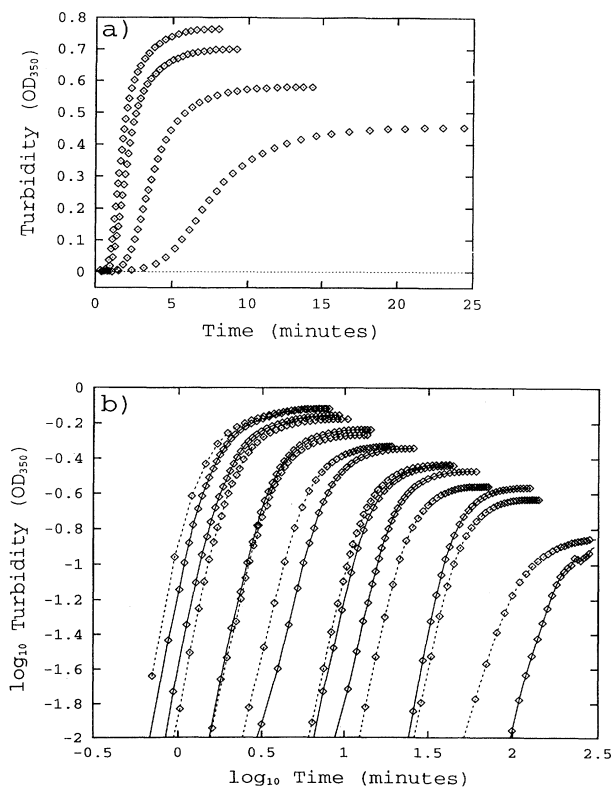


FIG. 3. Turbidity as a function of time for various tubulin concentrations, measured in terms of the optical density at 350 nm wavelength (OD_{350}). (a) A sample of data from [7]. (b) The entire data set from [7] replotted with logarithmic axes.

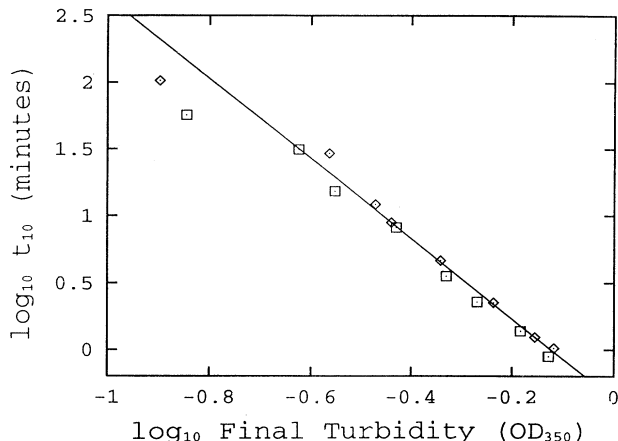


FIG. 4. Time required to reach $\frac{1}{10}$ of the final microtubule mass as a function of the final microtubule mass density. The line has a slope of -3 . The lack of correspondence with the two lowest mass densities is probably due to the limitations of the turbidity measurement, which is not reliable for microtubule mass densities below $0.2 \mu M$.

concentrations of the subcritical aggregates. It also becomes necessary to introduce a less trivial size dependence in the growth and shrinking probabilities of subcritical aggregates. In general, each aggregate of size i can have a unique g_i and s_i . In this slightly more complicated scenario, the microtubule mass can be expected to grow as

$$\frac{M(t)}{M_\infty} \propto C^N t^{i_c+1}, \quad (4)$$

where N is the number of dimers in the nucleus and i_c is the number of metastable subcritical aggregates.

Thus, from the power law measured in Fig. 3(b), we learn that abundant nucleation takes place in three or four steps and, combining that results with the scaling of the characteristic time, we estimate the size of the nucleus to be around 12 to 15 dimers.

B. Discussion

In their original analysis, Voter and Erickson interpreted their data in terms of a critical nucleus of 6–7 dimers [7]. The discrepancy arises because they fit to the entire time series and consequently compromise the goodness of the fit at early times. By addressing only the early time behavior, our analysis yields a better fit and, we believe, a more reliable interpretation. The lesson learned here may be applicable to studies of self-assembly in other biological systems as well [12].

Between the turbidity data and our own direct visualization, we have observed two different pathways of formation of the microtubule nucleus. We propose that it is the extent to which the system is quenched beyond the transition that determines which pathway is favored. However, besides the severity of the quench there is one major difference between the two experiments: glycerol.

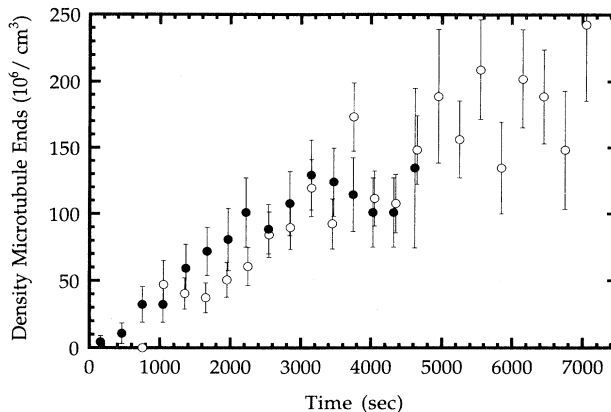


FIG. 5. Density of microtubule ends versus time with $3.4M$ glycerol in solution (open circles) ($C = 7.5 \mu M$ and $T = 21.5^\circ C$) and without (closed circles) ($C = 60 \mu M$ and $T = 18^\circ C$). Notice the sample with glycerol lasted about 20 min longer before saturating than the one without. This is consistent with our understanding that glycerol has a stabilizing effect [11].

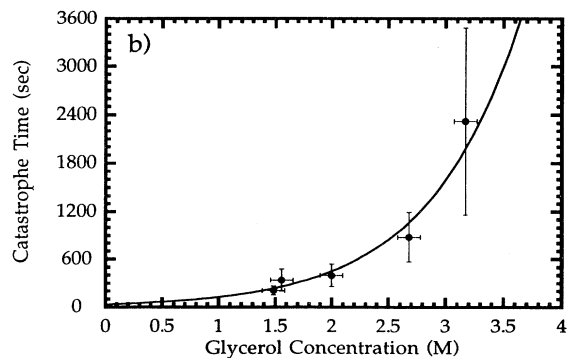
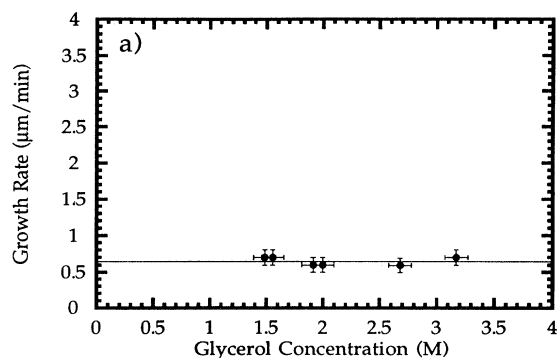


FIG. 6. Effects of glycerol on microtubule polymerization and dynamics. Measurements were made for $C = 13.5 \mu M$ and $T = 21.5^\circ C$. (a) Rate of microtubule elongation and (b) time between shortening events versus glycerol concentration. The large error bars in part (b) reflect low statistics.

IV. EFFECT OF GLYCEROL

It should not be overlooked that the two experiments discussed above employ different buffers. In the turbidity experiment, the buffer contained 50 mM MES, pH 6.6, 5 mM MgSO₄, 1 mM EGTA, 1 mM GTP, and 3.4M glycerol [7]. In the direct visualization experiment, the buffer contained 100 mM Pipes, pH 6.9, 2 mM MgSO₄, 2 mM EGTA, 1 mM GTP, and no glycerol [5]. The most significant difference is the presence of glycerol, which is commonly known to promote and stabilize microtubule formation [13]. Could it be that glycerol alone is responsible for the existence of the metastable subcritical aggregates observed in the deep quench?

To address this concern we introduced 3.4M glycerol in our buffer and repeated the marginal nucleation experiment. Figure 5 compares the time development of nucleation with glycerol (open circles) ($T=21.5^{\circ}\text{C}$ and $C=7.5\ \mu\text{M}$) and without (full circles) ($T=18^{\circ}\text{C}$ and $C=60\ \mu\text{M}$). Although it was necessary to drastically lower the concentration of tubulin to achieve conditions of marginal nucleation, we find the nucleation rate in the presence of glycerol is again constant in time. We therefore do not consider glycerol alone responsible for the different nucleation pathway found in the turbidity experiment. It is clear, however, that the presence of glycerol makes for a much deeper quench at a given temperature and tubulin concentration.

To understand how glycerol promotes spontaneous nucleation, we investigated its effect on microtubule polymerization and dynamic instability [8]. Our results are summarized in Fig. 6. Figure 6(a) shows that the rate of microtubule growth g is totally insensitive to the presence of glycerol. Instead, glycerol is effective in stabilizing microtubules against episodes of rapid shortening. As Fig. 6(b) shows, there is an exponential increase in the time between shortening events with increasing glycerol concentration. In terms of our simplest model, glycerol has the effect of increasing the ratio g/s by decreasing s . Going further, we suggest that these results indicate that glycerol reduces the rate of GTP hydrolysis which accompanies tubulin aggregation. It may be that hydrolysis plays a key role in destabilizing subcritical aggregates of tubulin, thereby limiting spontaneous assembly. These conjectures are supported by another experiment in which a nonhydrolyzable analog of GTP was used and observed to enhance nucleation [14].

V. SUMMARY

We have studied the process of spontaneous nucleation of microtubules under two extreme conditions.

First we found that in both cases the critical nucleus involves between 10 and 14 tubulin dimers. This range is strikingly similar to the range of microtubule protofilament numbers observed under the electron microscope [15]. We are prompted to speculate that nucleation involves wrapping an aggregate of dimers into a closed, cylindrical form. If there is a preferred angle for bending between dimers, the probability for closure may depend strongly on the size of the aggregate. The low

probability of forming large unstable aggregates will compete with the difficulty of closing (and thus stabilizing) small ones, to favor a particular sized aggregate for nucleation. As the quench deepens, g/s increases and this balance will shift to larger sizes. Therefore microtubules with larger numbers of protofilaments might be more common at deeper quenches.

Experiments have shown that the microtubule protofilament number is sensitive to buffer conditions [16]. We suggest that different buffer conditions may simply correspond to different quenches. This conjecture could be tested by systematically varying the severity of the quench (e.g., adjusting the concentration of tubulin or glycerol), and observing the number of protofilaments in the microtubules under the electron microscope.

Next, we found two significantly different pathways to assembly of the critical nucleus. Near the onset of spontaneous nucleation, we found a constant nucleation rate and concluded that the critical nucleus forms in a single step. Upon quenching to conditions far beyond onset, the nucleation rate increases with time and there exist three or four metastable states along the path to assembly of the critical nucleus. Finally, we have shown that the presence of glycerol deepens the quench and is not directly responsible for the stability of subcritical aggregates.

There appears to be a transition separating one-step nucleation from nucleation via metastable states. We have not yet gained access to the intermediate regime. We note that it should be possible to visualize the full range of nucleation pathways directly under the microscope if very thin ($\sim 1\ \mu\text{m}$) samples are used for the deep quenches. However, the question of control over the available tubulin concentration would have to be addressed with care.

ACKNOWLEDGMENTS

We are grateful to W. A. Voter and H. P. Erickson for sharing their data on the temporal evolution of turbidity in quenched solutions of tubulin. This work was supported by the National Science Foundation through Grant No. PHY-9408905. H.F. and K.S. acknowledge support from the Danish Natural Science Research Council under Grant Nos. 11-0244-1 and 11-0608-1, respectively. H.F. thanks the Isaac Newton Institute for its hospitality and Julie Damm's Studiefond for support. D.K.F. acknowledges support from the NSF through the Graduate Fellowship Program.

APPENDIX

We analyze the time dependence of microtubule nucleation, limiting ourselves to early times when nearly all tubulin is in dimer form. In principle, one can imagine many different paths and intermediate stages by which tubulin dimers may assemble to form microtubules. We assume that one such path dominates entirely. We also assume that every stage in the path is connected to the next stage by the addition of dimers only, though not necessarily by addition of only one dimer per stage. In other words, we assume the rate of passage between stages depends only on the dimer concentration (to some

power) and not on the concentration of any small aggregates. We denote the concentration of assembly products at stage i by c_i . Individual dimers are the zeroth stage and their concentration is c_0 . We define n_i as the number of dimers needed to pass from stage $i-1$ to stage i and denote the final stage, the critical aggregate, by i_c . The critical aggregate thus contains $N=1+n_1+n_2+\dots+n_{i_c}$ dimers, and once it is formed a microtubule starts to grow. With the above assumptions the assembly process may be described by

$$\frac{dc_i}{dt} = f_{i-1}c_{i-1}c_0^{n_i} - b_i c_i - f_i c_i c_0^{n_{i+1}} + b_{i+1}c_{i+1} \quad \text{for } i > 0. \quad (\text{A1})$$

Here f_i is the forward and b_i the backward rate constant. In the special case of $i=i_c$, this equation must include an additional term to account for the loss of nuclei as they turn into microtubules. The dimer concentration c_0 can be determined by conservation of tubulin mass. The addition of n_i dimers in one step is effectively a description of n_i fast steps, in each of which a dimer is added to form an unstable aggregate. The separation of the process into steps i reflects a separation of the long time spent at metastable states i and the very short time spent in any unstable configurations between the metastable states.

Initially all of the tubulin is in dimer form: c_0 equals the initial dimer concentration C , and $c_i=0$ for all $i > 0$. At early times the occupation of subsequent states is

minimal and decreases rapidly with size: $c_i \ll c_{i-1} \ll c_0$ for all i . We are therefore justified in neglecting the effect of backward reactions and depletion (e.g., $c_0=C$). Also at early times, depletion of a given state i by forward reactions will be insignificant compared to the input from state $i-1$. Thus

$$c_i \propto C^{1+n_1+n_2+\dots+n_i} t^i + O(t^{i+1}). \quad (\text{A2})$$

For a given path with i intermediate steps, the accumulated number of nucleation seeds of critical size N will be

$$\text{nucl}(t) \propto C^N t^{i_c}. \quad (\text{A3})$$

Since nucleated microtubules grow at a rate proportional to c_0 [2], the accumulated microtubule mass will be

$$M(t) \propto C^{N+1} t^{i_c+1}. \quad (\text{A4})$$

These are the main formulas in our analysis. They are applicable only at early times. As time passes, depletion becomes important and the occupation of intermediate states saturates. This happens gradually, leading finally to a constant microtubule mass $M_\infty = \lim_{t \rightarrow \infty} M(t)$ that depends on the initial dimer concentration C .

We note that, although the above route to nucleation assumes that only dimers are added between steps, identical scaling exponents are obtained when we allow aggregates of different sizes to merge. Such processes, however, are much less likely than one in which the abundant tubulin dimers are used.

-
- [1] M. Kirschner and T. Mitchison, *Cell* **45**, 329 (1986).
 [2] R. A. Walker, E. T. O'Brien, N. K. Pryer, M. F. Soboiero, W. A. Voter, and H. P. Erickson, *J. Cell Biol.* **107**, 1437 (1988).
 [3] P. M. Bayley, *J. Cell Sci.* **95**, 329 (1990), and references therein.
 [4] H. Flyvbjerg, T. Holy, and S. Leibler, *Phys. Rev. Lett.* **73**, 2372 (1994).
 [5] D. Kuchnir Fygenson, E. Braun, and A. Libchaber, *Phys. Rev. E* **50**, 1579 (1994).
 [6] M.-F. Carlier and D. Pantaloni, *Biochemistry* **17**, 1908 (1978).
 [7] W. A. Voter and H. P. Erickson, *J. Biol. Chem.* **259**, 10430 (1984).
 [8] D. Kuchnir Fygenson, Ph. D. thesis, Princeton University, 1995.
 [9] In samples less than 25 μm thick nonspecific absorption of tubulin on glass becomes significant and the tubulin concentration is not well controlled. A measurement of this effect is given in [5].
 [10] B. J. Berne, *J. Mol. Biol.* **89**, 737 (1974).
 [11] A parametrization of the microtubule length l to the turbidity

M^* at a wavelength of 0.35 μm scattered light gives $M^* \sim 200l^2$ for $l < 0.2 \mu\text{m}$ and $M^* \sim 60l - 4$ for $l > 0.2 \mu\text{m}$ (Appendix of [10]). The most sensitive case is the one with the fastest nucleation rate ($C = 19 \mu\text{M}$). In this case microtubules grow at a rate $v \approx 0.1 \mu\text{m}/\text{sec}$ and thus reach the linear regime in a time $\tau = 2$ sec after nucleation. Assuming the nucleation rate increases with time $R(t) \propto t^\alpha$, the turbidity at time t , integrated over all previous nucleation events, is $M^*(t) = \int_0^t R(t') M^*(l = v(t-t')) dt'$
 $pp [6/(\alpha+1)(\alpha+2)] t^{\alpha+2} - [4/(\alpha+1)] t^{\alpha+1} + 4\tau t^\alpha$ to lowest order in τ , where both t and τ are in seconds. The first term dominates once $t > 2(\alpha+2)/3$. For typical values of $\alpha \sim 3$, this happens when $t > 3$ sec.

- [12] P. E. Privilege, Jr., D. Thomas, and J. King, *Biophys. J.* **64**, 824 (1993).
 [13] E. T. O'Brien and H. P. Erickson, *Biochemistry* **28**, 1414 (1989).
 [14] A. A. Hyman, S. Salser, D. N. Dreschel, N. Unwin, and T. J. Mitchison, *Mol. Biol. Cell* **3**, 1155 (1992).
 [15] R. H. Wade and D. Chrétien, *J. Struct. Biol.* **110**, 1 (1993).
 [16] S. Ray, E. Meyhöfer, R. A. Milligan, and J. Howard, *J. Cell Biol.* **121**, 1083 (1993).